

**This item is the archived peer-reviewed author-version of:**

Time series modelling for wastewater-based epidemiology of COVID-19 : a nationwide study in 40 wastewater treatment plants of Belgium, February 2021 to June 2022

**Reference:**

Bertels Xander, Hanoteaux Sven, Janssens Raphael, Maloux Hadrien, Verhaegen Bavo, Delputte Peter, Boogaerts Tim, van Nuijs Alexander, Brogna Delphine, Linard Catherine, ....- Time series modelling for wastewater-based epidemiology of COVID-19 : a nationwide study in 40 wastewater treatment plants of Belgium, February 2021 to June 2022  
The science of the total environment - ISSN 1879-1026 - (2023), 165603  
Full text (Publisher's DOI): <https://doi.org/10.1016/J.SCITOTENV.2023.165603>  
To cite this reference: <https://hdl.handle.net/10067/1976850151162165141>

# TITLE PAGE

**Title:** Time series modelling for wastewater-based epidemiology of COVID-19: A nationwide study in 40 wastewater treatment plants of Belgium, February 2021 to June 2022

**Authors:** Xander Bertels<sup>1</sup> (0000-0002-4815-9067), Sven Hanoteaux<sup>2</sup>, Raphael Janssens<sup>2</sup> (0000-0002-4383-1053), Hadrien Maloux<sup>2</sup>, Bavo Verhaegen<sup>3</sup> (0000-0002-1709-5259), Peter Delputte<sup>4</sup> (0000-0003-3972-616X), Tim Boogaerts<sup>5</sup> (0000-0002-3802-3174), Alexander L.N. van Nuijs<sup>5</sup> (0000-0002-9377-6160), Delphine Brogna<sup>6</sup> (0000-0002-4354-4177), Catherine Linard<sup>6</sup> (0000-0002-0819-7755), Jonathan Marescaux<sup>6,7</sup>, Christian Didy<sup>8</sup>, Rosalie Pype<sup>8</sup> (0000-0002-8785-5946), Nancy H.C. Roosens<sup>9</sup> (0000-0001-9218-078X), Koenraad Van Hoorde<sup>3</sup>, Marie Lesenfants<sup>2</sup>, Lies Lahousse<sup>1</sup> (0000-0002-3494-4363)

## Affiliations

1. Department of Bioanalysis, Ghent University, 9000 Ghent, Belgium
2. Epidemiology and Public Health, Epidemiology of Infectious Diseases, Sciensano, 1050 Brussels, Belgium
3. Infectious Diseases in Humans, Foodborne Pathogens, Sciensano, 1050 Brussels, Belgium
4. Laboratory for Microbiology, Parasitology and Hygiene, University of Antwerp, 2610 Wilrijk, Belgium
5. Toxicological Centre, University of Antwerp, 2610 Antwerp, Belgium
6. Institute of Life, Earth and Environment, University of Namur, 5000 Namur, Belgium
7. E-BIOM SA, 5000 Namur, Belgium
8. Société Publique de Gestion de l'Eau, 4800 Verviers, Belgium
9. Biological Health Risks, Transversal Activities in Applied Genomics, Sciensano, 1050 Brussels, Belgium

**Corresponding author:** Lies Lahousse ([lies.lahousse@ugent.be](mailto:lies.lahousse@ugent.be)): Ottergemsesteenweg 460, 9000 Gent, Belgium

## Authors' contributions:

Study concept and design: XB, LL, SH, and CL. Sample collection, sample analyses, protocols, and data management: RJ, HM, BV, PD, TB, AvN, JM, CD, RP, NR, KVH, SH, and ML. Statistical methodology: XB, LL, and SH. Formal analysis: XB and SH. Drafting of the

34 manuscript: XB. Critical review of the manuscript: SH, RJ, HM, BV, PD, TB, AvN, DB, CL,  
35 JM, CD, RP, NR, KVH, ML, and LL. Supervision and management: LL and ML. All authors  
36 contributed to and approved the final version of the Article.

37 **Funding:** This work was supported by the Belgian Federal Government (grants COVID-  
38 19\_SC048, COVID-19\_SC063, and COVID-19\_SC093). It was also supported by Société  
39 Publique de Gestion de l'Eau (SPGE), E-BIOM, and the University of Namur (CR-280) through  
40 two public procurements (MP20.051, MP20.097). SPGE was involved in wastewater sampling  
41 and communication of data regarding the Walloon WWTPs. E-BIOM was involved in  
42 wastewater analysis. Both SPGE and E-BIOM contributed to the co-authoring review process  
43 of the paper. Yet the funders had no role in the design of the study, in the interpretation of data,  
44 in drafting the manuscript, or in the decision to publish the results.

45 **Conflicts of interest:** None declared

46 **Ethical statement:** Ethical approval was not needed for this study. Detection of SARS-CoV-2  
47 RNA in wastewater provides anonymised data. Aggregated clinical data was used and is  
48 publicly available (<https://epistat.sciensano.be/covid/>).

49

50 **Data availability:** Clinical datasets are publicly available (<https://epistat.sciensano.be/covid/>).  
51 Wastewater data is partially available online (<https://epistat.wiv-isp.be/covid/covid-19.html>). R  
52 script are available upon reasonable request.

53

#### 54 **Abbreviations:**

- 55 - AICc: corrected Akaike Information Criterion
- 56 - IE: inhabitant equivalent
- 57 - IQR: interquartile range
- 58 - LOQ: limit of quantification
- 59 - NSD: normalised standard deviation
- 60 - PMMoV: pepper mild mottle virus
- 61 - RMSE: root-mean-square error
- 62 - RNA: ribonucleic acid
- 63 - SD: standard deviation
- 64 - WBE: wastewater-based epidemiology
- 65 - WWTPs: wastewater-treatment plants

66

## ABSTRACT

67 **Background:** Wastewater-based epidemiology (WBE) has been implemented to monitor surges of  
68 COVID-19. Yet, multiple factors impede the usefulness of WBE and quantitative adjustment may be  
69 required.

70 **Aim:** We aimed to model the relationship between WBE data and incident COVID-19 cases, while  
71 adjusting for confounders and autocorrelation.

72 **Methods:** This nationwide WBE study includes data from 40 wastewater treatment plants (WWTPs) in  
73 Belgium (02/2021-06/2022). We applied ARIMA-based modelling to assess the effect of daily flow  
74 rate, pepper mild mottle virus (PMMoV) concentration, a measure of human faeces in wastewater, and  
75 variants (alpha, delta, and omicron strains) on SARS-CoV-2 RNA levels in wastewater. Secondly,  
76 adjusted WBE metrics at different lag times were used to predict incident COVID-19 cases. Model  
77 selection was based on AICc minimization.

78 **Results:** In 33/40 WWTPs, RNA levels were best explained by incident cases, flow rate, and PMMoV.  
79 Flow rate and PMMoV were associated with -13.0% (95% prediction interval: -26.1 to +0.2%) and  
80 +13.0% (95% prediction interval: +5.1 to +21.0 %) change in RNA levels per SD increase, respectively.  
81 In 38/40 WWTPs, variants did not explain variability in RNA levels independent of cases. Furthermore,  
82 our study shows that RNA levels can lead incident cases by at least one week in 15/40 WWTPs. The  
83 median population size of leading WWTPs was 85.1% larger than that of non-leading WWTPs. In 17/40  
84 WWTPs, however, RNA levels did not lead or explain incident cases in addition to autocorrelation.

85 **Conclusion:** This study provides quantitative insights into key determinants of WBE, including the  
86 effects of wastewater flow rate, PMMoV, and variants. Substantial inter-WWTP variability was  
87 observed in terms of explaining incident cases. These findings are of practical importance to WBE  
88 practitioners and show that the early-warning potential of WBE is WWTP-specific and needs validation.

89

90 **Keywords:** wastewater surveillance; COVID-19; ARIMA; PMMoV; flow rate

91 **Abstract word count: 288**

93 

## 1 Introduction

94 Accurate monitoring of community-wide severe acute respiratory syndrome coronavirus 2 (SARS-CoV-  
95 2) spread is vital to estimate and reduce the societal impact of coronavirus disease (COVID-19). To this  
96 end, individual clinical testing has been used extensively to diagnose COVID-19 infections and impose  
97 quarantine measures (Vandenberg et al., 2021). Yet it is costly and has a tendency to be biased towards  
98 symptomatic infections due to ineffective detection of asymptomatic cases (Girum et al., 2020). Hence,  
99 for epidemiological monitoring, wastewater-based epidemiology (WBE) of SARS-CoV-2 has been  
100 implemented as a complementary surveillance tool (Agrawal et al., 2021; Janssens et al., 2022; Rainey  
101 et al., 2022; Rector et al., 2023). WBE is a method that enables detection of faecally and urinary excreted  
102 SARS-CoV-2 genes in influent wastewater to monitor viral surges (Anand et al., 2021; Anand et al.,  
103 2022; Cevik et al., 2021; Park et al., 2021) and has an early-warning potential (Mao et al., 2020; Shah  
104 et al., 2022). Additional advantages of WBE to clinical testing are its capability to detect both  
105 symptomatic and asymptomatic infections (Parasa et al., 2020), to provide more inclusive, privacy-  
106 friendly, and population-wide estimates, and allow more targeted clinical testing (Amman et al., 2022).

107 Nonetheless, the potential of WBE remains limited due to important variability in WBE estimates caused  
108 by the complexity of influent wastewater samples, external factors such rainfall and chlorination, and  
109 heterogeneity of wastewater treatment plants (WWTPs) and sewer networks. Hence, a myriad of factors  
110 affect the measured viral gene concentrations, including wastewater dilution, wastewater composition,  
111 and population factors such as variability in viral shedding and uncertainty in the size of the underlying  
112 population represented in a given wastewater sample (Bertels et al., 2022; Li et al., 2023). Therefore,  
113 the true number of viral RNA copies per resident remains unknown.

114 Adjusting for those key determinants, including flow rate, wastewater faecal strength, and population  
115 size, have been proposed to improve the utility of WBE estimates (Bertels et al., 2022). Yet, there is  
116 little research assessing the quantitative effects of these phenomena on viral concentrations in  
117 wastewater (Vallejo et al., 2022), which is critical to decide how to adjust for these factors. Although  
118 WBE estimates can be highly correlated to clinical cases of COVID-19 (D'Aoust et al., 2021; Vallejo et  
119 al., 2022; Westhaus et al., 2021), to the best of our knowledge there has been no study to date which  
120 optimizes the wastewater metric by adjusting for those factors to quantitatively model COVID-19 cases.

121 In this nationwide WBE study, wastewater was sampled twice weekly over more than one year  
122 (02/2021-06/2022) at 40 WWTPs in Belgium covering more than five million inhabitants. We aimed (i)  
123 to model the effect of flow rate, human faecal loads, and variants (alpha, delta, and omicron strains) on  
124 wastewater SARS-CoV-2 RNA levels and (ii) to optimize wastewater metrics to explain incident  
125 COVID-19 cases. Our study shows that wastewater flow rate and population dynamics, but not variants,

126 consistently explain RNA levels independent of cases. We provide meta-analysed effect sizes and  
127 prediction intervals, allowing other researchers to adjust RNA levels independent from incident cases.  
128 Furthermore, we show that WBE can lead clinical epidemiology by one week, but only in a minority of  
129 WWTPs due to substantial inter-WWTP variability. Lastly, we found that in some WWTPs RNA levels  
130 were not informative for incident cases in addition to autocorrelation of cases.

## 131 2 Material and methods

### 132 2.1 Data description

#### 133 2.1.1 Wastewater data

134 Influent wastewater samples were collected at 40 Belgian wastewater treatment plants (WWTPs)  
135 covering approximately 5 million inhabitants, which represents 43% of the Belgian population (Figure  
136 1 and Table S1). In the context of national wastewater surveillance, 24h samples are collected twice a  
137 week on Monday and Wednesday. Results from 15 February 2021 to 8 June 2022 were used in this  
138 study. During this period, quantitative SARS-CoV-2 RNA concentrations were obtained using a  
139 consistent protocol. Nucleocapsid 1 (N1), nucleocapsid 2 (N2) and envelope (E) RNA copies of SARS-  
140 CoV-2 were used as markers of viral presence in wastewater. Wastewater analyses were performed by  
141 Sciensano (Belgian public health institution), by the University of Antwerp and by E-BIOM (spin-off  
142 from the University of Namur) (Table S1), using the methods from Boogaerts et al. (2021 and Coupeau  
143 et al. (2020. A detailed overview of the sample collection, concentration, extraction, and PCR-based  
144 quantification is presented in the Supplementary File.

145 In each of the WWTPs, the covered population size was defined as the census-based domestic inhabitant  
146 equivalent, normalised by the geographical catchment area (Table S1) and the flow rate was measured  
147 by flowmeter as the daily incoming flow rate divided by 24h (m<sup>3</sup>/h). Pepper mild mottle virus (PMMoV)  
148 RNA copy concentration, as indicator of human faeces in wastewater, was measured during the same  
149 period and used as a proxy for the number of people present in a catchment area. PMMoV is an  
150 extremely stable plant virus that infects plants from the *Capsicum* genus (pepper-containing food  
151 products) and shows widespread abundance in human stool and wastewater, without strong seasonal  
152 fluctuation (Rosario et al., 2009; Zhang et al., 2006).

#### 153 2.1.2 Epidemiological data

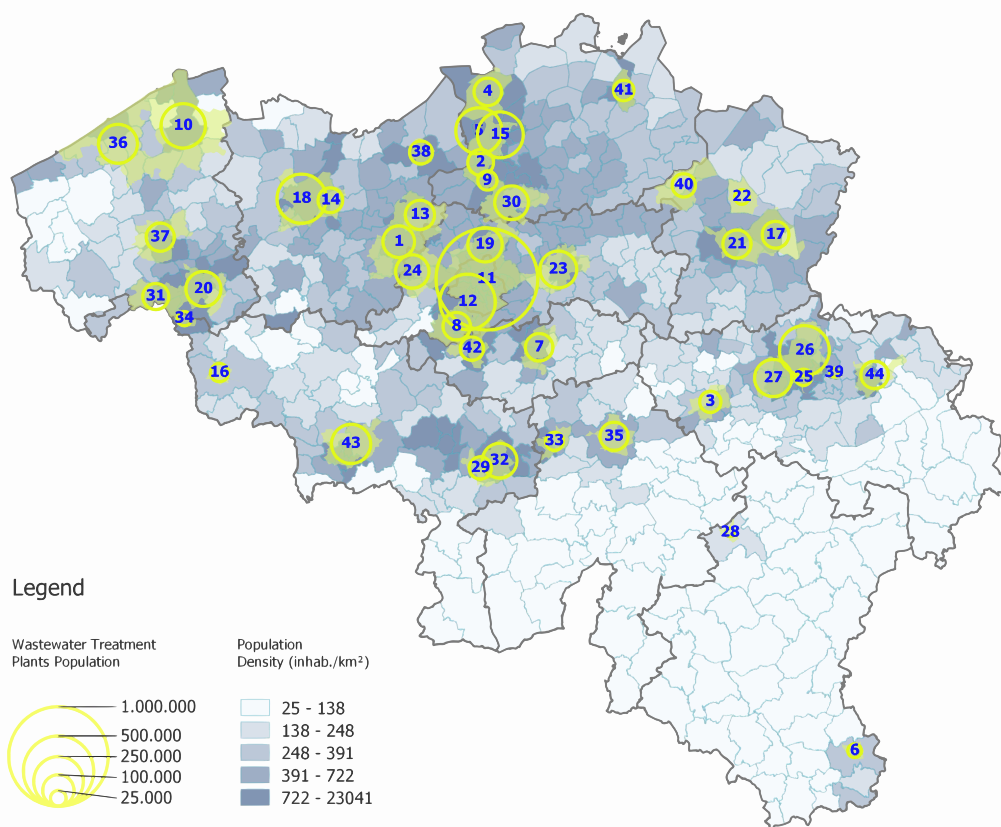
154 The number of incident COVID-19 cases for a given WWTP was defined as the total daily number of  
155 positive COVID-19 PCR tests at the corresponding municipality normalised by the fraction of the  
156 covered municipality inhabitant equivalent by the WWTP catchment area.

157 The spread of SARS-CoV-2 has been characterised by several variants. As these variants could have an  
158 impact on the link between the epidemiological situation and the evolution of the viral concentrations  
159 in wastewater, they need to be accounted for. Data on variants circulating in the Belgian population were  
160 provided by the COVID-19 Genomics Belgium Consortium (Cuypers et al., 2022). During the period  
161 considered in this study, a variant was defined as dominant when its proportion was equal to or higher  
162 than 50%. Hence, the period under study has been divided into three subcategories depending on which  
163 variant was dominant: from 15 February 2021 to 14 June 2021, Alpha was dominant; from 21 June 2021

164 to 12 December 2021, Delta was dominant and from 27 December 2021 to 8 June 2022, Omicron was  
165 dominant.

### 166 2.1.3 Data sources, missing data and data transformation

167 All data sources are reported in the Supplementary File. For both the SARS-CoV-2 and the PMMoV  
168 RNA concentrations, concentration replicates below the limit of quantification (LOQ) of 20 copies/mL  
169 were coded as half of the LOQ (10 copies/mL) and negative replicates were coded as 1 copy/mL to  
170 allow for logarithmic transformation (Ma, 2020). To explore the link between the epidemiological  
171 situation and the viral concentrations in wastewater, additional wastewater metrics have been defined:  
172 (i) the PMMoV mass load (copies/day) is defined as the PMMoV concentration (copies/mL) x flow rate  
173 (mL/day); (ii) the viral mass load (copies/day) is defined as the SARS-CoV-2 RNA concentration  
174 (copies/mL) x flow rate (mL/day) and the viral to PMMoV ratio (-) is defined as the SARS-CoV-2 RNA  
175 concentration (copies/mL) / PMMoV concentration (copies/mL). Finally, both the viral concentration  
176 and the viral mass load were logged as +1. Missing wastewater data (1.3%) was replaced by an estimate  
177 obtained through time-dependent linear interpolation. Missing data and negative results for each  
178 treatment plant were listed in Table S2.



179  
180 **Figure 1.** Map of Belgium with the location and coverage of 44 WWTPs used in the national wastewater  
181 surveillance program (Janssens et al., 2022) and municipality population density. Catchment areas are  
182 indicated by yellow surface colour. Four WWTPs were excluded from this analysis due to no available  
183 data (WWTP of Boom (nr. 9)) or shorter data coverage (WWTP of Liège Grosses Battes (nr. 25)),



184 Soumagne (nr. 39), and Wegnez (nr. 44)) due to flooding events in July 2021. The numerical population  
185 size coverage of each WWTP is shown in Table S1. (Color print.)

186

## 187 2.2 Statistical analysis

### 188 2.2.1 Modelling wastewater SARS-CoV-2 RNA levels

189 Non-seasonal autoregressive integrated moving average (ARIMA) models and dynamic regression were  
190 applied to model SARS-CoV-2 RNA concentrations (Hyndman and Athanasopoulos, 2021). Briefly,  
191 ARIMA models are a type of time series models which describe autocorrelation. Dynamic regression  
192 models are (multiple) regression models extended with ARIMA. Dynamic regression models used in  
193 this study have a similar coefficient interpretation as standard regression but allow integrating the  
194 autocorrelation structure of the data. A comprehensive discussion of these model types is presented in  
195 the Supplementary File.

196 The logarithm ( $\log_{10}$ ) of wastewater SARS-CoV-2 RNA concentration, defined as the average  
197 concentration of N1-, N2-, and E-gene RNA copies, was modelled. For every WWTP, an ARIMA model  
198 and 8 dynamic regression models were fitted. Dynamic regression models were adjusted for  
199  $\log_{10}$ (COVID-19 cases) and with combinations of the following predictors (Table S3): (i) daily flow rate  
200 ( $\text{m}^3/\text{h}$ ), (ii) PMMoV concentration (copies/L) or PMMoV mass load (copies/day), and (iii) dichotomous  
201 predictors of SARS-CoV-2 variants (alpha, delta, and omicron strains), based on 50% or higher  
202 prevalence of sequenced clinical samples.

### 203 2.2.2 Modelling incident COVID-19 cases

204 Incident  $\log_{10}$ (cases) were modelled by an ARIMA model and dynamic regression models, which  
205 included one of the following wastewater metric combinations: viral concentrations (copies/mL), viral  
206 mass load (copies/day), viral to PMMoV ratio (-), or viral mass load and viral to PMMoV ratio. Each of  
207 the four combinations was tested with the wastewater metrics lagged up to 2 weeks (i.e., up to 4 distinct  
208 sampling dates). This resulted in 16 dynamic regression models. All the dynamic regression models  
209 used the dichotomous predictors of the variants as a covariate. An exhaustive list of the considered  
210 models is presented in Table S4.

### 211 2.2.3 Model selection and meta-analysis

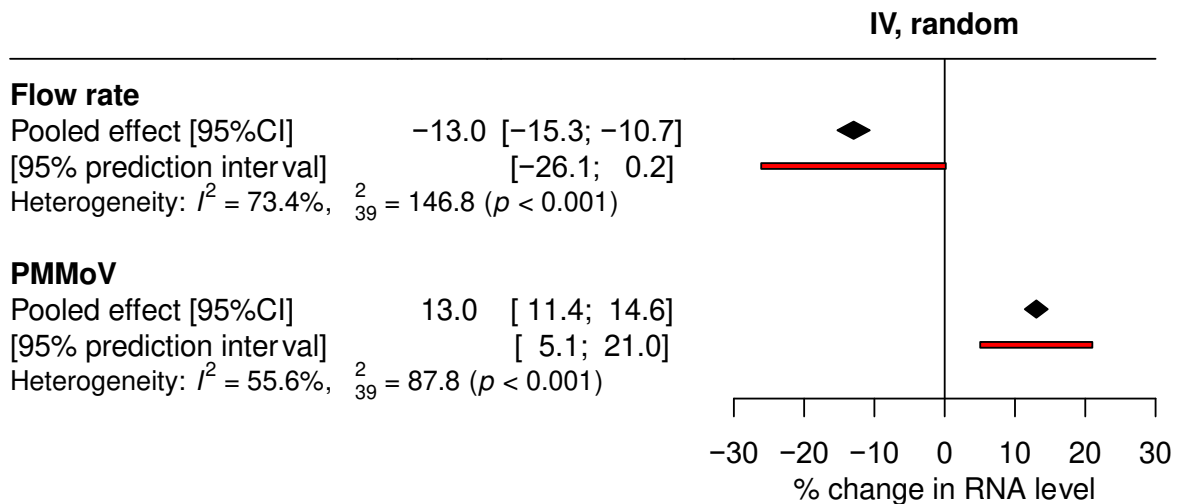
212 The optimal ARIMA specification of the models was set in a data-driven way by non-stepwise corrected  
213 Akaike Information Criterion (AICc) minimization, and with a first order of differencing ( $d = 1$ ) to  
214 account for non-stationarity (Hyndman and Athanasopoulos, 2021; Kwiatkowski et al., 1992). Once the  
215 optimal ARIMA specification was obtained for each of the proposed model structures, the best model  
216 for a given WWTP was selected based on AICc scores, as a measure of predictive accuracy. The most  
217 selected RNA model was fitted on all WWTPs, and effect sizes were meta-analysed by a random-effects

218 model using inverse-variance weighting. The root-mean-square error (RMSE), a goodness-of-fit  
219 indicator, of the selected model was compared to a standard multiple regression model based on  
220 backward stepwise selection. All analyses were performed in R 4.0.5 (Vienna, Austria) using the  
221 forecast package for the ARIMA models and all data visualization was done with the ggplot2 package  
222 (Hyndman et al., 2022; Hyndman and Khandakar, 2008; R Core Team, 2022; Wickham, 2016).

223 **3 Results**

224 **3.1 Determinants of SARS-CoV-2 RNA levels in wastewater**

225 In 33/40 WWTPs a dynamic regression model of  $\log_{10}(\text{cases})$ , wastewater flow rate and PMMoV  
 226 concentration was selected as the most accurate model to explain wastewater SARS-CoV-2 RNA levels  
 227 (Table S5). This model was applied on all WWTPs and effect sizes were meta-analysed. One standard  
 228 deviation (SD) increase in flow rate was associated with 13.0% (95% prediction interval (95%PI): -26.2  
 229 to +0.2%) decrease in RNA levels, independent of cases and PMMoV (Figure 2). Reversely, one SD  
 230 increase in PMMoV levels was associated with 13.0% (95%PI: +5.1 to +21.0%) increase in RNA levels,  
 231 independent of cases and flow rate (Figure 2). The removal of flow rate, PMMoV, or both variables  
 232 from this model significantly reduces the predictive accuracy (median  $\Delta\text{AICc}$ : +10.9, +12.8, and +27.5,  
 233 respectively, Table S6). Independent of flow rate and PMMoV, a 10.0% increase in incident cases was  
 234 associated with 4.5% (95%PI: +1.0 to 8.0%) increase in RNA levels. Overall, the best models explained  
 235 on average 64.7% ( $R^2$ , SD = 10.4%) of the variation in RNA levels. Detailed meta-analyses for flow  
 236 rate and PMMoV are presented in the Supplementary File (Figures S1-2).



237  
 238 **Figure 2. Meta-analysis of the independent effect of flow rate and pepper mild mottle virus**  
 239 **(PMMoV) on SARS-CoV-2 RNA levels in wastewater, adjusted for incident cases. Effect sizes are**  
 240 **expressed as percentage change in RNA level per one standard deviation increase in flow rate and**  
 241 **PMMoV, respectively.**

242  
 243 In 35/40 WWTPs, increasing flow rate was associated with a statistically significant drop in wastewater  
 244 RNA levels, independent of cases and PMMoV. Exceptions were the WWTPs of Houthalen Centrum,  
 245 Marchienne-au-Pont, Vallée du Hain (l'Orchis), Montignies-sur-Sambre and Wasmuel (Figure S1). In  
 246 the latter WWTP, a nominal positive trend was observed (+4.7% (95%CI: -2.2 to +11.5%)). The optimal  
 247 model for this WWTP did not include additive flow rate adjustment, although implicitly included

248 through correction for PMMoV mass load (copies/day). The WWTP of Wasmuel was the 8<sup>th</sup> largest  
249 catchment area in terms of covered population size in this study and showed the lowest normalised  
250 standard deviation (NSD) of flow rate (0.21) and the second smallest NSD of PMMoV (0.55).

251 In 36/40 WWTPs, increasing PMMoV was associated with a statistically significant increase in RNA  
252 levels, adjusted for cases and flow. Exceptions were the WWTPs of Tessenderlo, Turnhout, Hasselt, and  
253 Mouscron-versant-Espierres (Figure S2). In the former three WWTPs, no SARS-CoV-2 RNA was  
254 detected (i.e., RNA concentration below the limit of detection) for a substantial number of dates (Table  
255 S2). In the latter WWTP (Mouscron-versant-Espierres), wastewater was collected from both the Belgian  
256 (~21,200 IE) and France (~120,000 IE) population. Collection of French wastewater represented a  
257 substantial flow which was not covered in the clinical testing surveillance. Three out of five of the most  
258 impacted treatment plants included large student campuses (UC Louvain (Basse-Wavre), University of  
259 Liège (Liège Oupeye), and KU Leuven (Leuven)).

260 Lastly, an intercept for dominant variants improved the model accuracy only in 2/40 WWTPs  
261 (Destelbergen and Marchienne-au-Pont). In those two WWTPs, RNA levels of SARS-CoV-2 were 71%  
262 lower during the delta wave (B.1.617.2 strain) and 69% lower during the omicron waves (BA.1, BA.2,  
263 BA.2.75, BA.2+L452X, and BA.4 strains) compared to the period when the alpha variant (B.1.1.7) was  
264 dominant for a given number of cases, and adjusted for flow rate and PMMoV levels.

265 In 38/40 WWTPs, the selected dynamic regression model showed a lower RMSE value than the optimal  
266 standard multiple regression model. Overall, the average RMSE difference of dynamic regression  
267 models was 3.9 times lower than those of standard multiple regression models (Table S9).

268

## 269 3.2 Wastewater-based surveillance data to model incident COVID-19 cases

### 270 3.2.1 Optimal wastewater metric to link incident COVID-19 cases

271 In 28/40 WWTPs, the optimal model for incident COVID-19 cases included wastewater-based  
272 surveillance data. In the remaining 12/40 WWTPs, a standard ARIMA model, which does not include  
273 wastewater information, outperformed dynamic regression models in terms of predictive accuracy  
274 (Table 1a).

275 Of the 28 models that included a WBE metric, a flow-adjusted viral mass load was included in 15/28  
276 WWTPs (Table 1a), while a viral-to-PMMoV gene ratio was included in 8/28 WWTPs. Overall, the  
277 flow-adjusted mass load was selected in larger WWTPs (87,633 (IQR = 102,225) vs 78,290 (IQR =  
278 68,030) IE) while viral-to-PMMoV gene ratio was selected in smaller WWTPs (67,077 (IQR = 63,443)  
279 vs 82,082 (IQR = 92,296) IE) in terms of population coverage.

280 An unadjusted and unlagged viral concentration was selected in 2 of the 28 WWTPs (WWTPs of  
 281 Aartselaar and Tessenderlo). These WWTPs were modestly sized WWTPs (68,031 and 55,546 vs  
 282 82,156 (IQR = 85,479) IE) and showed large variability in log(RNA) levels (0.46 and 0.82 vs 0.29 (IQR  
 283 = 0.12) NSD) and in PMMoV mass load (1.31 and 1.10 vs 0.76 (IQR = 0.29) NSD).

284 **Table 1.** Optimal models to link wastewater data with incident COVID-19 cases.

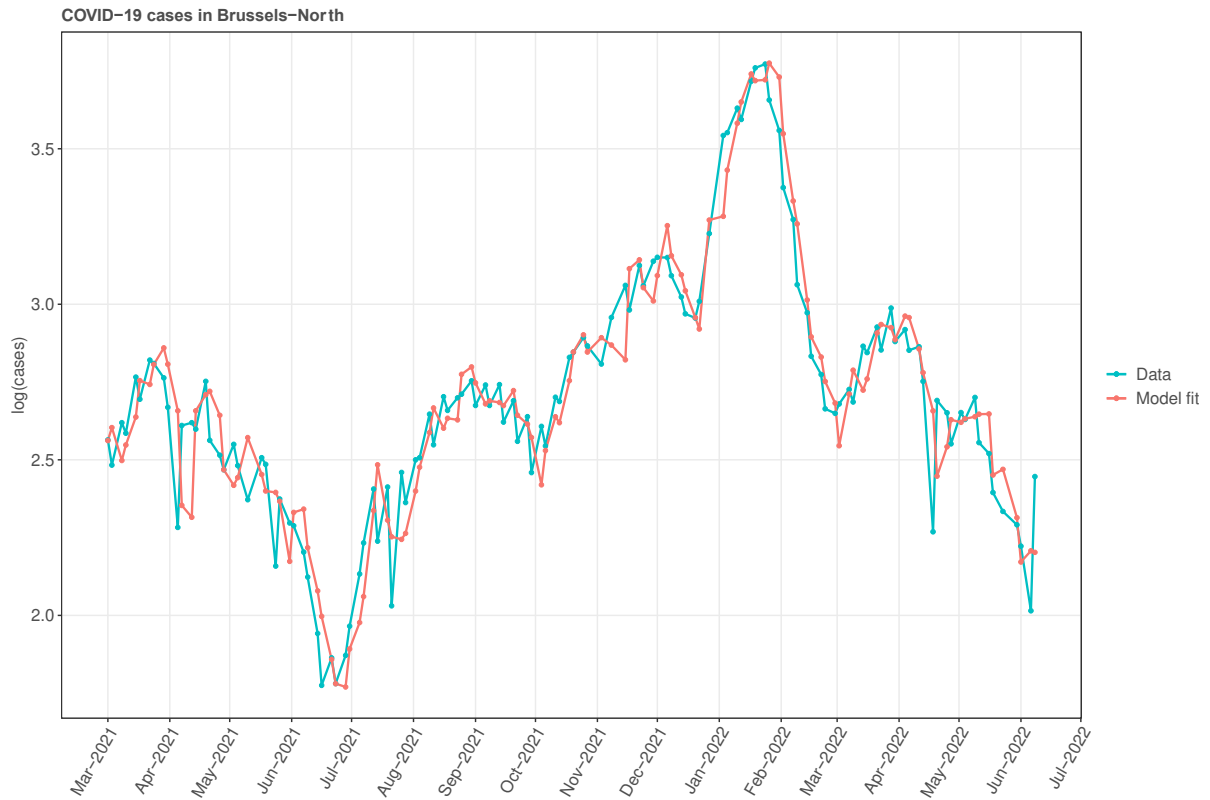
<b>A) Optimal wastewater metric (n = 40)</b>	
<b>WWTPs (n)</b>	<b>Metric</b>
12/40	No wastewater metric*
7/40	Unadjusted viral concentration
13/40	Viral mass load
6/40	Viral-to-PMMoV ratio
2/40	Viral mass load + viral-to-PMMoV ratio
<b>B) Optimal lag time of wastewater metric (n = 28)</b>	
<b>WWTPs (n)</b>	<b>Lag time</b>
5/28	Unlagged wastewater metric
8/28	1-sample leading wastewater metric
10/28	2-sample leading wastewater metric (1 week)
3/28	3-sample leading wastewater metric
2/28	4-sample leading wastewater metric (2 weeks)

285 Viral concentration = SARS-CoV-2 RNA copies/mL; viral mass load = flow-adjusted SARS-CoV-2  
 286 RNA copies per day; viral-to-PMMoV ratio = SARS-CoV-2 gene copies per PMMoV gene copy.  
 287 \*Dynamic regression models with ARIMA-modelled errors were applied, except when no wastewater  
 288 metric was included (standard ARIMA). Dynamic regression models adjusted for dominance of alpha,  
 289 delta, or omicron variants (dichotomously coded (0/1) depending on dominant prevalence ( $\geq 50\%$  of  
 290 samples)).

291

### 292 3.2.2 Early-warning potential of wastewater metric

293 Among the 28 catchment areas, a leading wastewater indicator of at least one week showed the best  
 294 predictive accuracy in 15/28 WWTPs, with the one-week leading indicator being selected in most  
 295 (10/28) treatment plants (Table 1b, Table S7). The median covered population size in leading WWTPs  
 296 was 85.1% larger than in those where a non-leading wastewater indicator was selected (102,800 (IQR  
 297 66,735) vs 55,546 (IQR = 33,891) IE). The coefficients of all 28 models are presented in Table S8. A  
 298 sensitivity analysis using correlation coefficients (Table S7) showed similar results in 12/28 WWTPs, a  
 299 more pronounced lead time in 8/28 WWTPs, and a less pronounced lead time in 8/28 WWTPs. Figure  
 300 3 illustrates the optimal model (1-week leading viral mass load) at the largest WWTP (Brussels-North,  
 301 1,045,900 IE) to explain incident cases of COVID-19.



302

303 **Figure 3.** Logarithm of incident COVID-19 cases (blue) at the largest WWTP (Brussels-North, covering  
 304 approximately one million inhabitants) and predicted incident cases based on a model including the one-  
 305 week leading viral mass load (RNA copies/day) (red). Model diagnostics are presented in Figure S3.  
 306 (Color print.)

## 307 4 Discussion

308 This nationwide study modelled the relationship between wastewater-based SARS-CoV-2 RNA levels  
309 and incident COVID-19 cases, covering approximately 5 million Belgian inhabitants for more than one  
310 year. This is the first study to show the relative effect size of wastewater flow rate and PMMoV  
311 concentrations on SARS-CoV-2 RNA levels in wastewater, while accounting for autocorrelation.  
312 Secondly, SARS-CoV-2 variants did not explain variability of RNA levels for a given number of cases  
313 in the large majority of WWTPs (38/40). Furthermore, different WBE metrics were tested at different  
314 lag times for subsequent use in monitoring COVID-19 epidemiology. This study confirms that WBE  
315 data can lead incident cases by at least one week but only in a minority of WWTPs (15/40). In 17/40  
316 WWTPs, different wastewater metrics did not lead or explain incident cases in addition to  
317 autocorrelation. Future studies should therefore validate the early-warning potential of WWTPs and  
318 investigate whether WBE adds beyond autocorrelation to support the additional efforts/costs of  
319 determining RNA levels at these areas/WWTPs for predicting incident cases.

320 This analysis showed that increasing daily flow rate reduces RNA levels by on average -13.0% per SD  
321 increase, independent of incident cases and PMMoV (e.g., dilution by rainfall and other sources  
322 including industrial water and drain water). Flow-adjusted viral mass loads approach viral dynamics  
323 more accurately, which was demonstrated through its empirical support in our incident case models.  
324 Viral mass loads were mainly selected in WWTPs serving larger populations.

325 Secondly, our results validate that PMMoV is a key contributor to RNA variability, independent of cases  
326 and flow. Higher PMMoV levels were associated with increasing viral RNA levels and may serve as a  
327 proxy for the number of persons contributing to a wastewater sample. This is reinforced by the  
328 observation that the PMMoV was not selected in the station of Mouscron-versant-Espierres, where the  
329 cases are not truly linked with the represented population. Also, PMMoV may be used as a normalization  
330 standard for additional variability which is not explicitly defined in the models. Unmeasured phenomena  
331 such as RNA adsorption, aqueous-solid phase distribution and degradation may be implicitly modelled,  
332 partly, by normalizing for PMMoV. RNA of SARS-CoV-2 will likely be affected in similar ways as  
333 PMMoV RNA due to their common physicochemical properties of RNA including molecule size and  
334 stability, overall negative charge, and as substrates of RNases. The ratio of viral-to-PMMoV gene copies  
335 improved case models in about one in five WWTPs. A lower number of inhabitants was covered in these  
336 WWTPs, presumably increasing the relevance of relative changes in population size. In contrast,  
337 PMMoV levels did not associate with viral RNA levels in five smaller WWTPs in which the dynamic  
338 of the viral evolution was not connected with the true underlying population due to for example zero-  
339 inflation of the viral concentrations. To allow more model flexibility, one may need a normalization  
340 marker for in-sewage factors and a different marker to account for the underlying population size and  
341 dynamics of a catchment area (e.g., mobility data from telecom providers).

342 In 38/40 WWTPs, additively correcting for the dominant SARS-CoV-2 strain did not improve model  
343 predictive accuracy for RNA levels. Hence, faecal shedding kinetics of SARS-CoV-2 variants were  
344 likely stable over time. This suggests that increasing infectiousness of variants may be caused by  
345 increased infectiousness of viral particles and/or selective respiratory shedding but was not associated  
346 with increased faecal shedding. In the two WWTPs with an informative variant term, less RNA was  
347 detected for a given number cases in the delta and omicron waves compared to the alpha wave.  
348 Importantly, shedding kinetics may be affected by increasing immunity among the population over time  
349 (Puhach et al., 2022).

350 Finally, this study demonstrates that, although different WWTPs share common dynamical  
351 characteristics, every WWTP has its particular dynamic in time as demonstrated by the amplitude of the  
352 measured effect sizes within the same model structure, this for both the flow rate and the PMMoV  
353 concentrations. The diversity of dynamics unravelled in this study thus shows that care must be taken  
354 when comparing RNA levels measured at different WWTP and that aggregation of quantitative data in  
355 a fixed effect model should be avoided. Aggregation and comparison are still possible but should be  
356 paired with a normalization process and/or using indicators (3). Also, additional factors which were not  
357 accounted for in this study, including the organic load and the number of solid particles in sewage,  
358 wastewater pH, and water chlorination will contribute to the remaining unexplained variability (~ 35%)  
359 (Bertels et al., 2022; Li et al., 2021).

360 The main strengths of this study were the nationwide population scale, the large number and  
361 heterogeneity of WWTPs, the long duration (> 1 year), and the high resolution of the data (twice-weekly  
362 sampling). Secondly, this study was performed during a period with the highest frequency of diagnostic  
363 COVID-19 tests in Belgium (Sciensano, 2023). Lastly, through ARIMA-based modelling, we accounted  
364 for autocorrelation enabling in-depth inferences of effect sizes. The added value of dynamic regression  
365 models was corroborated by its superior accuracy compared to standard multiple regression models in  
366 this context.

## 367 **Limitations**

368 A main limitation is the potential of model misspecification due to additional factors influencing RNA  
369 levels in wastewater and the true number of incident cases. Some of these factors are challenging to  
370 quantify (RNA degradation and testing strategy bias during the study period). Another main limitation  
371 is the uncertainty of the underlying population size. Capturing population dynamics may require other  
372 more accurate ways, for example through mobile data records or other big data sources (Deville et al.,  
373 2014). However, PMMoV showed to be of added value to tackle both the issue of standardization and  
374 population dynamics. Thirdly, vaccination coverage was not included in this analysis, which may have  
375 a profound effect on viral shedding (Puhach et al., 2022). As the effect of vaccination is time-dependent,  
376 we assume that it is implicitly accounted for through ARIMA-modelling of the residuals. However, its



377 effects cannot be quantitatively deduced from this study. Fourthly, variant strains were based on clinical  
378 samples and not on wastewater detection of variants. Finally, we used unevenly spaced time series which  
379 complicates the interpretation of lag times.

380

381 Future work should adjust for population dynamics, consider inter-WWTP variability, and may  
382 overcome some of the limitations of this research by using additional quantitative data sources such as  
383 vaccination coverage and mobility data, and by considering other epidemiological outcomes such as  
384 hospitalizations. Additionally, future studies should investigate spatiotemporal variation in the lead  
385 time, including the effect of seasonality, variant strains, and changes in shedding kinetics.

386

## 387 5 Conclusions

388 This study provides quantitative insights into the effect of key determinants to reduce unexplained  
389 variability of wastewater-based epidemiology (WBE). Adjusting for daily flow rate and PMMoV  
390 (population dynamics), but not variants, substantially improves COVID-19 modelling by WBE.  
391 Secondly, our findings show that WBE can lead individual clinical testing by one week, yet important  
392 heterogeneity between catchment areas was observed. This shows that the early-warning potential of  
393 WBE needs to be validated on a WWTP-specific level.

## 394 6 Acknowledgement

395 We would like to acknowledge Aquiris, Aquafin, Hydria and the Walloon approved sanitation  
396 organisations (AIDE, IDEA, IDELUX, IGRETEC, INASEP, inBW and IPALLE) for  
397 contributing to this project.

398 7 References

399 Agrawal S, Orschler L, Lackner S. Long-term monitoring of SARS-CoV-2 RNA in wastewater of the  
400 Frankfurt metropolitan area in Southern Germany. *Sci Rep* 2021; 11: 5372.

401 Amman F, Markt R, Endler L, Hupfauf S, Agerer B, Schedl A, et al. Viral variant-resolved wastewater  
402 surveillance of SARS-CoV-2 at national scale. *Nat Biotechnol* 2022; 40: 1814-1822.

403 Anand U, Adelodun B, Pivato A, Suresh S, Indari O, Jakhmola S, et al. A review of the presence of  
404 SARS-CoV-2 RNA in wastewater and airborne particulates and its use for virus spreading  
405 surveillance. *Environ Res* 2021; 196: 110929.

406 Anand U, Li X, Sunita K, Lokhandwala S, Gautam P, Suresh S, et al. SARS-CoV-2 and other pathogens  
407 in municipal wastewater, landfill leachate, and solid waste: A review about virus surveillance,  
408 infectivity, and inactivation. *Environ Res* 2022; 203: 111839.

409 Bertels X, Demeyer P, Van den Bogaert S, Boogaerts T, van Nuijs ALN, Delputte P, et al. Factors  
410 influencing SARS-CoV-2 RNA concentrations in wastewater up to the sampling stage: A  
411 systematic review. *Sci Total Environ* 2022: 153290.

412 Boogaerts T, Jacobs L, De Roeck N, Van den Bogaert S, Aertgeerts B, Lahousse L, et al. An alternative  
413 approach for bioanalytical assay optimization for wastewater-based epidemiology of SARS-  
414 CoV-2. *Sci Total Environ* 2021; 789: 148043.

415 Cevik M, Tate M, Lloyd O, Maraolo AE, Schafers J, Ho A. SARS-CoV-2, SARS-CoV, and MERS-  
416 CoV viral load dynamics, duration of viral shedding, and infectiousness: a systematic review  
417 and meta-analysis. *Lancet Microbe* 2021; 2: e13-e22.

418 Coupeau D, Burton N, Lejeune N, Loret S, Petit A, Pejakovic S, et al. SARS-CoV-2 Detection for  
419 Diagnosis Purposes in the Setting of a Molecular Biology Research Lab. *Methods Protoc* 2020;  
420 3.

421 Cuypers L, Dellicour S, Hong SL, Potter BI, Verhasselt B, Vereecke N, et al. Two Years of Genomic  
422 Surveillance in Belgium during the SARS-CoV-2 Pandemic to Attain Country-Wide Coverage  
423 and Monitor the Introduction and Spread of Emerging Variants. *Viruses* 2022; 14.

424 D'Aoust PM, Mercier E, Montpetit D, Jia JJ, Alexandrov I, Neault N, et al. Quantitative analysis of  
425 SARS-CoV-2 RNA from wastewater solids in communities with low COVID-19 incidence and  
426 prevalence. *Water Res* 2021; 188: 116560.

427 Deville P, Linard C, Martin S, Gilbert M, Stevens FR, Gaughan AE, et al. Dynamic population mapping  
428 using mobile phone data. *Proc Natl Acad Sci U S A* 2014; 111: 15888-93.

429 Girum T, Lentiro K, Geremew M, Migora B, Shewamare S. Global strategies and effectiveness for  
430 COVID-19 prevention through contact tracing, screening, quarantine, and isolation: a  
431 systematic review. *Trop Med Health* 2020; 48: 91.

432 Hyndman R, Athanasopoulos G. *Forecasting: Principles and Practice: OTexts*, 2021.

433 Hyndman R, Athanasopoulos G, Bergmeir C, Caceres G, Chhay L, O'Hara-Wild M, et al. *forecast:*  
434 *Forecasting functions for time series and linear models*, 2022.

435 Hyndman RJ, Khandakar Y. Automatic Time Series Forecasting: The forecast Package for R. *Journal*  
436 *of Statistical Software* 2008; 27.

437 Janssens R, Hanoteaux S, Maloux H, Klamer S, Laisnez V, Verhaegen B, et al. SARS-CoV-2  
438 Surveillance in Belgian Wastewaters. *Viruses* 2022; 14: 1950.

439 Kwiatkowski D, Phillips PCB, Schmidt P, Shin Y. Testing the null hypothesis of stationarity against the  
440 alternative of a unit root. *Journal of Econometrics* 1992; 54: 159-178.

441 Li X, Zhang S, Sherchan S, Orive G, Lertxundi U, Haramoto E, et al. Correlation between SARS-CoV-  
442 2 RNA concentration in wastewater and COVID-19 cases in community: A systematic review  
443 and meta-analysis. *J Hazard Mater* 2023; 441: 129848.

444 Li X, Zhang S, Shi J, Luby SP, Jiang G. Uncertainties in estimating SARS-CoV-2 prevalence by  
445 wastewater-based epidemiology. *Chem Eng J* 2021; 415: 129039.

446 Ma J. Estimating epidemic exponential growth rate and basic reproduction number. *Infect Dis Model*  
447 2020; 5: 129-141.

448 Mao K, Zhang K, Du W, Ali W, Feng X, Zhang H. The potential of wastewater-based epidemiology as  
449 surveillance and early warning of infectious disease outbreaks. *Curr Opin Environ Sci Health*  
450 2020; 17: 1-7.

451 Parasa S, Desai M, Thoguluva Chandrasekar V, Patel HK, Kennedy KF, Roesch T, et al. Prevalence of  
452 Gastrointestinal Symptoms and Fecal Viral Shedding in Patients With Coronavirus Disease  
453 2019: A Systematic Review and Meta-analysis. *JAMA Netw Open* 2020; 3: e2011335.

454 Park SK, Lee CW, Park DI, Woo HY, Cheong HS, Shin HC, et al. Detection of SARS-CoV-2 in Fecal  
455 Samples From Patients With Asymptomatic and Mild COVID-19 in Korea. *Clin Gastroenterol*  
456 *Hepatol* 2021; 19: 1387-1394 e2.

457 Puhach O, Meyer B, Eckerle I. SARS-CoV-2 viral load and shedding kinetics. *Nat Rev Microbiol* 2022:  
458 1-15.

459 R Core Team. *R: A Language and Environment for Statistical Computing*, Vienna, Austria, 2022.

460 Rainey AL, Loeb JC, Robinson SE, Lednicky JA, McPherson J, Colson S, et al. Wastewater surveillance  
461 for SARS-CoV-2 in a small coastal community: Effects of tourism on viral presence and variant  
462 identification among low prevalence populations. *Environ Res* 2022; 208: 112496.

463 Rector A, Bloemen M, Thijssen M, Delang L, Raymenants J, Thibaut J, et al. Monitoring of SARS-  
464 CoV-2 concentration and circulation of variants of concern in wastewater of Leuven, Belgium.  
465 *J Med Virol* 2023; 95: e28587.

466 Rosario K, Symonds EM, Sinigalliano C, Stewart J, Breitbart M. Pepper Mild Mottle Virus  
467 as an Indicator of Fecal Pollution. *Applied and Environmental Microbiology* 2009; 75: 7261-7267.

468 Sciensano. Dashboard COVID-19 Epidemiological Situation Belgium, 2023.

469 Shah S, Gwee SXW, Ng JQX, Lau N, Koh J, Pang J. Wastewater surveillance to infer COVID-19  
470 transmission: A systematic review. *Sci Total Environ* 2022; 804: 150060.

471 Vallejo JA, Trigo-Tasende N, Rumbo-Feal S, Conde-Perez K, Lopez-Oriona A, Barbeito I, et al.  
472 Modeling the number of people infected with SARS-COV-2 from wastewater viral load in  
473 Northwest Spain. *Sci Total Environ* 2022; 811: 152334.

474 Vandenberg O, Martiny D, Rochas O, Van Belkum A, Kozlakidis Z. Considerations for diagnostic  
475 COVID-19 tests. *Nature Reviews Microbiology* 2021; 19: 171-183.

476 Westhaus S, Weber FA, Schiwy S, Linnemann V, Brinkmann M, Widera M, et al. Detection of SARS-  
477 CoV-2 in raw and treated wastewater in Germany - Suitability for COVID-19 surveillance and  
478 potential transmission risks. *Sci Total Environ* 2021; 751: 141750.

479 Wickham H. *ggplot2: Elegant Graphics for Data Analysis*. New York: Springer-Verlag, 2016.

480 Zhang T, Breitbart M, Lee WH, Run JQ, Wei CL, Soh SW, et al. RNA viral community in human feces:  
481 prevalence of plant pathogenic viruses. *PLoS Biol* 2006; 4: e3.